

Article

Computational Investigation of Co-Solvent Influence on CO₂ Absorption and Diffusion in Water Lean Solvents

Maimoona Sharif ¹, Chunliang Ge ², Tao Wang ^{1,*}, Wei Zhang ², Mengxiang Fang ¹ and Xiang Gao ¹

¹ State Key Laboratory of Clean Energy Utilization, Zhejiang University, Hangzhou 310027, China

² Zhejiang Zheneng Technology & Environment Group Co., Ltd., Hangzhou 310003, China

* Correspondence: oatgnaw@zju.edu.cn

Abstract: The present research explores water-lean amine-based solvents to enhance carbon capture and provide sustainable solutions for CO₂ emissions challenges. A computational approach is employed to evaluate the co-solvent's impact on CO₂ capture in MDEA-based systems. The performance of the following systems is examined: MDEA-NMP, MDEA-MAE-NMP, MDEA-MeOH, MDEA-MAE-MeOH, MDEA-EG, MDEA-MAE-EG, and MDEA-MAE with varying water concentrations. The Radial Distribution Function (RDF) analysis revealed significant interactions between amine groups, CO₂, and water molecules in each system. The results indicate that the MDEA-NMP (40%H₂O) and MDEA-EG (40%H₂O) systems had strong interactions, indicating their potential for CO₂ capture. However, adding MAE decreased interaction intensities, indicating a less favorable performance. Complementing the RDF findings, the Mean Square Displacement (MSD) analysis quantified CO₂ diffusivity across temperatures (313 K, 323 K, and 333 K). MDEA-NMP (40%H₂O) demonstrated the highest diffusivity, indicating superior CO₂ mobility and capture efficiency. MDEA-MeOH (40%H₂O) also showed moderate diffusivity, further supporting its effectiveness. However, solvent systems incorporating MAE consistently displayed lower diffusivity, reinforcing the observation from the RDF analysis. The temperature effect on the diffusivity of selected blends does not follow the regular pattern in a co-solvent-based system, whereas in an aqueous system, it increases with temperature. These molecular dynamic simulations highlight the critical role of solvent composition in optimizing CO₂ capture efficiency. Applying these insights can improve solvent formulations, enhance effectiveness, and reduce costs.



Citation: Sharif, M.; Ge, C.; Wang, T.; Zhang, W.; Fang, M.; Gao, X. Computational Investigation of Co-Solvent Influence on CO₂ Absorption and Diffusion in Water Lean Solvents. *Processes* **2024**, *12*, 1588. <https://doi.org/10.3390/pr12081588>

Academic Editor: Carla Silva

Received: 21 June 2024

Revised: 17 July 2024

Accepted: 24 July 2024

Published: 29 July 2024



Copyright: © 2024 by the authors. Licensee MDPI, Basel, Switzerland. This article is an open access article distributed under the terms and conditions of the Creative Commons Attribution (CC BY) license (<https://creativecommons.org/licenses/by/4.0/>).

1. Introduction

Carbon capture, utilization, and storage (CCUS) involves various technologies designed to capture and store carbon dioxide (CO₂) emissions from industrial processes and power plants. Within the broader framework of CCUS applications, chemical absorption using amine-based solvents is one of the well-established methods for capturing CO₂ among several approaches and is widely employed [1,2]. In 2020, China set ambitious targets to peak its carbon emissions by 2030 and reach carbon neutrality by 2060 [3–5]. CCUS is an essential element for this target. Utilizing absorption systems, particularly those employing amine solutions commonly adopted in industrial settings, offers the advantages of rapid CO₂ absorption rates and high CO₂ removal efficiency. However, the inherent challenges posed by the high corrosivity of these solvents and the considerable energy consumption associated with the process have placed limitations on large-scale industrial CO₂ capture [6]. In recent years, scholarly research and development has shifted towards exploring novel chemical absorption systems by water-lean solvents [7]. This shift is accompanied by an emphasis on optimizing absorption and regeneration processes [1]. There are numerous investigations [8–11] on water-lean solvents. Replacing water with organic solvents in absorbents has shown notable benefits, such as lower regeneration energy

needs and reduced corrosiveness and degradation [12–15]. Recent literature has explored a variety of organic compounds, including alcohols such as methanol, ethanol, propanol, and butanol [11], glycols like ethylene glycol and their mixtures [16], dimethylformamide [17], and 1-methyl-2-pyrrolidone [18], etc. This has driven significant advancements in developing nonaqueous or semi-aqueous absorbents by blending secondary amines with organic co-solvents.

In a water-lean solvent, water is partially replaced with an organic co-solvent, reducing the overall water concentration in the blend. Maintaining an appropriate water balance is essential for the long-term sustainability of CO₂ capture technology [19]. Some co-solvents can significantly reduce the viscosity of the solvent mixture, making it easier to handle and improving the kinetics of CO₂ absorption. Lower viscosity facilitates better flow and mixing in industrial applications, which is critical for large-scale CO₂ capture processes [20]. The other advantage of the co-solvent is that it can enhance the solubility of CO₂ in the solvent system. This is particularly true for solvents that have specific interactions with CO₂, such as hydrogen bonding or Lewis acid-base interactions. For example, certain glycols and glycol ethers have been shown to increase the CO₂ solubility in water-lean systems [9,20]. Co-solvents can improve the thermal stability of the solvent mixture, making the system more robust under the high temperatures typically required for solvent regeneration. This ensures that the solvent can be reused multiple times without significant degradation, thus reducing operational costs [9,20]. Table 1 illustrates the evolution of absorbents. The composition of absorbents has evolved from first-generation single-component amine solvents to second-generation amine blend solutions and third-generation absorbents with improved capture capability and more diversified components. Table 1 shows that the regeneration energy consumption of absorbents has dropped from 4.0 GJ·ton⁻¹ CO₂ to 1.8–2.4 GJ·ton⁻¹ CO₂, greatly lowering capture costs.

Table 1. Historical development of amine-based absorbents.

Generation	Type of Solvents	Energy Consumption (GJ/tCO ₂)	Advantages	Disadvantages	Reference
1st Generation 1930s	Amine Solvents 30 wt% MEA PZ aqueous solvents	3.7–4.0	Fast reaction rate High capture capacity	High energy penalty solvent regeneration	[21]
2nd Generation 1990s	Blended amine solvent	2.5–3.2	Improved capture efficiency Low energy compared to single amine	Possible increased volatility and corrosiveness depending on the blend	[22]
3rd Generation 2000s	Water-lean solvent/Phase-change Absorbent	1.8–2.4	Lower overall energy consumption compared to aqueous amine systems Lower water content reduce energy consumption for regeneration Enhanced selectivity and capacity for CO ₂ capture	Higher viscosity can lead to mass transfer limitations Limited long term operation data available	[23]

The capture procedure with amine absorbents involves reacting CO₂ with the absorbent in the absorption unit. The CO₂-enriched solution is heated and transferred to the desorption unit, decomposing into CO₂ at high temperatures [24]. The solution is then chilled before being reintroduced to the absorption device to react further with flue gas. This approach necessitates transporting all solutions to the desorption device and adding heat to vaporize the water, resulting in high capture costs and limited CO₂ absorption

capability [8]. Researchers investigated several amine solutions to lower capture costs by optimizing capture methods, adjusting absorbent concentrations, utilizing different solvents, and changing reaction conditions. An ideal absorbent should have a fast CO₂ reaction rate, a large absorption capacity, low operating costs, good thermal stability, economic feasibility, and environmental compatibility [25]. To overcome the limits of single-component amine solvents, researchers have created novel absorbents such as amine-blended absorbents, ionic liquid absorbents, phase-change absorbents, and water-lean absorbents that increase capture performance while lowering costs [21–23]. Extensive research has delved into their absorption characteristics, physical properties, and kinetics in both solvent-free and aqueous conditions for CO₂ capture [9,26–28]. Table 2 shows the list of selected solvents in the present study. In our investigation, we blended pure MDEA (N-methyldiethanolamine) and a combination of MDEA and MAE 2-(methylamino) ethanol) with three other co-solvents, NMP, EG, and MeOH. The selection of these solvents is based on the numerous advantages mentioned in the literature.

Table 2. List of solvents selected in the present study.

Name	Molecular Structure	Molecular Weight (g·mol ⁻¹)	Density (g·mL ⁻¹)	CAS No.
MDEA		119	1.1	105-59-9
MeOH		32	0.80	67-56-1
MAE		75	0.94	109-83-1
EG		64	1.1	107-21-1
NMP		99	1.03	872-50-4

NMP has a high solubility in CO₂, which improves absorption effectiveness. It also retains thermal stability, which is necessary for efficient regeneration processes [29]. NMP serves as the solvent reducing energy consumption, attributable to its low heat capacity, vaporization enthalpy, and high chemical stability [30]. Methanol has been thoroughly researched for CO₂ capture applications because of its high solubility and low viscosity, which promote greater mass transfer, and its high volatility, which makes regeneration easier [31]. Ethylene glycol is an effective CO₂ absorber due to its potent hydrogen bonding properties with CO₂ and low vapor pressure, which minimize solvent losses [32]. These solvents are selected based on their suitability for a range of process circumstances in addition to their unique qualities.

Similarly, MDEA is a tertiary amine known for its high capacity to absorb CO₂ in both aqueous and water-lean solvents [26,27]. It is widely used in gas treatment processes because of its efficiency in capturing CO₂ from natural gas and other industrial emissions [26]. MDEA is particularly advantageous because it can selectively remove CO₂, making it ideal for high-selectivity applications. MAE, a secondary amine, is highly effective in CO₂ capture due to its high reactivity with CO₂. It forms carbamate complexes quickly, which is beneficial in environments where rapid CO₂ absorption is needed [21]. MAE is often combined with other amines to enhance the overall CO₂ absorption efficiency and stability of the solvent system [28]. The combination of MDEA and MAE leverages the strengths of both solvents. MDEA provides high CO₂ absorption capacity with lower energy re-

quirements for regeneration, while MAE offers fast reaction kinetics. This synergistic effect results in a solvent system that is both efficient and cost-effective for CO₂ capture.

This study explores three critical aspects of solvent-based CO₂ capture, focusing on the solvent system MDEA-MAE with MeOH, NMP, and EG. Previous research has largely focused on pure solvents and amine blends, leaving a gap in understanding the effects of various co-solvents and diffusivity rates in these specific mixtures. This research aims to fill this gap by investigating the effect of co-solvents in pure MDEA and blended MDEA-MAE and diffusion rate estimation with three different organic co-solvents. This study makes substantial contributions to current research through three key components: firstly, investigating the effects of co-solvents on CO₂ absorption in both pure MDEA-NMP, MDEA-EG, and MDEA-MeOH and blended systems (MDEA-MAE-NMP, MDEA-MAE-EG, and MDEA-MAE-MeOH) using molecular dynamics (MD) simulations; secondly, analyzing the diffusivity rate and effect of temperature on the diffusivity of various types of innovative water-lean systems; and thirdly, integrating simulation models to evaluate the impact of different co-solvents and diffusion rates. The ultimate objective is to identify the most effective amines for laboratory-scale application to reduce atmospheric carbon emissions and lessen environmental impact.

2. Modelling Approach and Reaction Mechanism

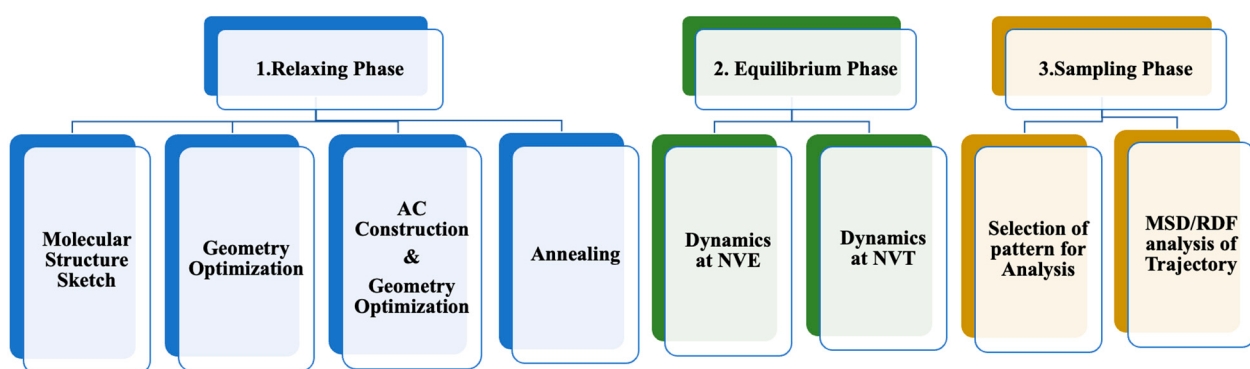
Molecular Dynamics (MD) simulations were utilized to examine molecular interactions at a microscopic level in an amorphous environment. These simulations provide detailed insights into the dynamic behavior of particles by solving classical equations of motion [33,34]. The simulations were executed on a high-performance computer cluster with 64 processing cores to ensure efficiency and enable parallel computations. Key simulation parameters included the atom-based summation for geometry optimization, the Ewald summation for equilibrium and production phases, the COMPASS force field for interatomic potential calculations, and the velocity Verlet algorithm for time integration [35,36]. The Verlet algorithm was chosen for its numerical stability and time-reversible properties, allowing precise calculations with longer time steps. The COMPASS force field, optimized for condensed-phase atomic simulations, is suitable for solvent systems [35]. Table 3 provides the calculation for simulation model construction in the material studio, and Figure 1 shows the technical route adopted in the present research.

Table 3. Calculation for input parameters in the material studio.

System	Descriptions	MDEA	NMP	CO ₂	H ₂ O
MDEA-NMP (40Wt%H ₂ O)	Density of mixture (g.mL ⁻¹)	1.053			
	No. of molecules	12	10	11	111
	Weight%	30%	20%	10%	40%
MDEA-MeOH (40Wt%H ₂ O)	Descriptions	MDEA	MeOH	CO ₂	H ₂ O
	Density of mixture (g.mL ⁻¹)	1.007			
	No. of molecules	120	310	220	2220
MDEA-EG (40Wt%H ₂ O)	Weight%	30%	20%	10%	40%
	Descriptions	MDEA	EG	CO ₂	H ₂ O
	Density of mixture (g.mL ⁻¹)	1.067			
System MDEA-MAE-NMP (30%H ₂ O)	No. of molecules	44	54	40	80
	Weight%	30%	20%	10%	40%
	Descriptions	MDEA	MAE	NMP	CO ₂
	Density of mixture (g.mL ⁻¹)	1.044			
	No. of molecules	25	13	20	22
	Weight%	30%	10%	20%	10%
					166
					30%

Table 3. Cont.

System	Descriptions	MDEA	NMP	CO ₂	H ₂ O
MDEA-MAE-MEG (30%H ₂ O)	Descriptions	MDEA	MAE	MEG	CO ₂
	Density of mixture (g.mL ⁻¹)	1.058			H ₂ O
	No. of molecules	252	133	312	222
MDEA-MAE-MeOH (30%H ₂ O)	Weight%	30%	10%	20%	10%
	Descriptions	MDEA	MAE	MeOH	CO ₂
	Density of mixture (g.mL ⁻¹)	1.002			H ₂ O
MDEA-MAE-H ₂ O (50%H ₂ O)	No. of molecules	12	6	30	11
	Weight%	30%	10%	20%	10%
	Descriptions	MDEA	MAE		CO ₂
	Density of mixture (g.mL ⁻¹)	1.04			H ₂ O
	No. of molecules	25	13		22
	Weight%	30%	10%		10%

**Figure 1.** Steps of the research methodology adopted in the present work.

The MD simulation comprised four main steps: defining and optimizing molecular structures for CO₂ absorption studies, constructing the simulation environment with periodic boundary conditions, running an equilibrium phase (NVE ensemble) for 200 picoseconds followed by a production phase (NVT ensemble) with 1 femtosecond time steps (1 ns), and analyzing trajectory data, particularly the Radial Distribution Function (RDF), to understand molecular interactions (refer to Equation (1)) [35,37]. Guidance for calculations, including RDF and Mean Square Displacement (MSD) analysis, was provided by Biovia Material Studio software as well as from previous studies [38,39].

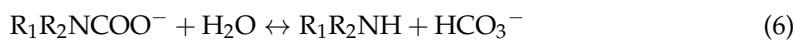
$$g(r) = \frac{1 < N(r, r + dr) >}{\rho 4\pi r^2 dr} \quad (1)$$

Following geometry optimization, the annealing process addressed the non-uniform molecular distribution within the amorphous cell, ensuring a realistic system representation. The combined energy minimization and annealing procedure, known as “relaxing the structure”, enhances the reliability and validity of simulations involving amorphous materials. The MSD typically exhibits two distinct behaviors: minimal diffusion with constant MSD during short times due to confinement and a linear increase in MSD over longer times as molecules move through free-volume pockets. The rise in MSD over time is directly linked to the diffusion coefficient (D) [40], as presented in Equations (2) and (3).

$$MSD = \langle r^2(t) \rangle = \left\langle \frac{1}{N} \sum_{i=0}^N (r_i(t) - r_i(0))^2 \right\rangle \quad (2)$$

$$D = \frac{1}{6} \lim_{t \rightarrow \infty} \frac{d}{dt} (\text{MSD}) \quad (3)$$

In the practical approach, various parameters influence the reaction between the amine and CO₂, including the type of absorbent, interactions between different amines, amine solution concentration, and temperature. The fundamental chemical reaction occurs between the amino group of the amine molecule and CO₂. Primary and secondary amines react with CO₂ to produce carbamates and protonated amines. Tertiary amines, on the other hand, cannot react directly with CO₂; instead, they require water to assist CO₂ hydrolysis, which results in bicarbonates [41]. The studies show that NMP, EG, and MeOH do not participate in chemical reactions with amines but react physically in water-lean solvents [7,32,42–44]. Therefore, we suppose that the co-solvents are present in the system but do not participate in chemical reactions. The interaction between CO₂ and primary/secondary amines has three major stages: carbamate formation, bicarbonate formation, and carbamate reversion. Equations (4)–(6) represent these steps [45]:



Carbamate production takes precedence when there is an excess of primary or secondary amines. In these circumstances, 0.5 moles of CO₂ and 1 mole of these amines can react to generate carbamates. All amines, however, may also experience some carbamate hydrolysis, suggesting that the absorbent may actually absorb more CO₂ than the 0.5 mole limit. In the presence of water, tertiary amines react with CO₂ via a base-catalyzed hydration process. This is due to the fact that tertiary amines do not have a CO₂-direct reactive site. Water makes it easier for CO₂ to hydrate and for bicarbonates to form. Equations (7) and (8) represent the reaction mechanism.



3. Model Validation

Evaluating amine density in molecular dynamics (MD) simulations is essential for assessing the performance of the selected force field. This computational approach calculates the density of amines in the simulated system, using the force field to provide insights into their molecular packing structure. To validate the accuracy of these simulations, the estimated density values are often compared with experimental data.

Table 4 facilitates this validation by presenting the densities of specific amines at standard conditions (298 K and 1 atm), serving as a reference for MD results. The simulations were conducted using the NPT ensemble over a 2 ns timescale, with data recorded every 5000 steps. The average density profiles, depicted in Figure 2a–c, visually represent the fluctuations in the densities of various pure amines such as MDEA, DEA, NMP, MeOH, and MEG, as well as blended amines like MDEA-MAE-EG, MDEA-EG, MDEA-MAE-MeOH, MDEA-MeOH, MDEA-MAE-NMP, MDEA-NMP, and MDEA-MAE within different regions of the simulation cell. These profiles (Figure 2) shed light on the density fluctuations throughout the simulation period at given conditions. The lines in Figure 2b are drawn to show the trend. The density of molecules depends on the number of molecules inserted in the simulation box. For pure substances, a higher molecular weight can contribute to a higher density. However, this relationship is not always straightforward due to the influence of molecular structure and intermolecular forces on molecular packing. A similar pattern is observed in the case of MAE; the simulation density is increased (Table 4). Stronger intermolecular forces, such as hydrogen bonds and van der Waals forces, can lead to tighter packing of molecules, thereby increasing density. For instance,

2-methylaminoethanol (MAE) exhibits significant hydrogen bonding due to its structure's amino and hydroxyl groups. Despite their relatively small molecular weight (75 g/mol), the ability of MAE molecules to form multiple hydrogen bonds results in a highly organized and tightly packed molecular structure. This extensive hydrogen bonding network significantly enhances the density of MAE, similar to how water, a small molecule, has a relatively high density due to its hydrogen bonding capabilities [46]. The hydrogen bonding can be a cause of the reduction in diffusivity observed in the present system. Because the organized and tightly packed molecules increase the viscosity and, as a result, decrease the diffusivity [46].

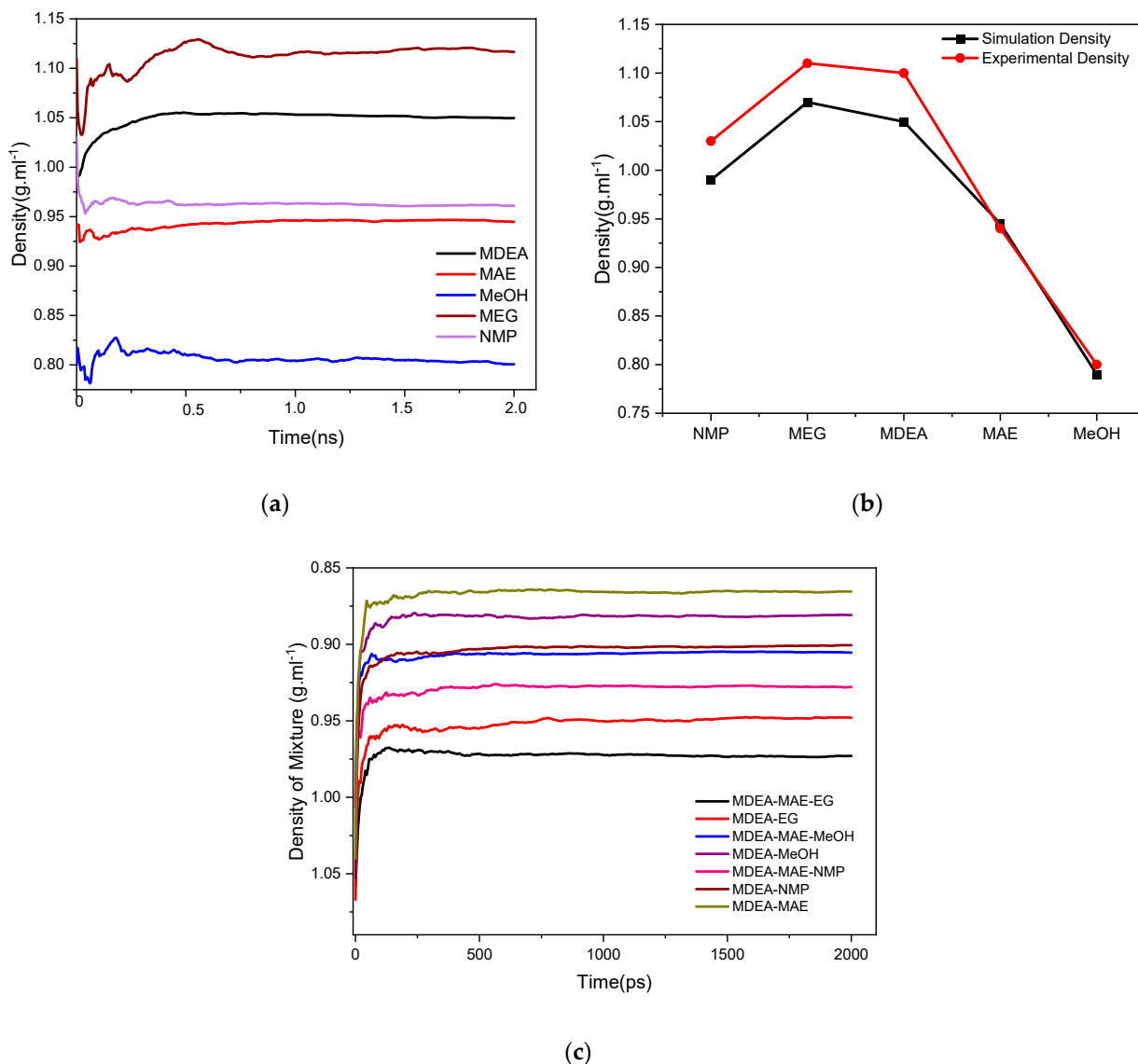


Figure 2. (a) Density estimation (g.mL^{-1}) for pure solvents in the present work; (b) comparison between simulation and experimental density (g.mL^{-1}) [47,48] of selected solvents; (c) density estimation (g.mL^{-1}) for mixtures.

Another crucial parameter to validate the force field and model employed in the study is periodic boundary conditions (PBCs). PBCs play a significant role in both the implementation and validation of simulations. They replicate an infinite system within a finite, imaginary simulation cell, ensuring a uniform distribution throughout the simulation process. Table 3 demonstrates that the simulation results align well with the experimental data, confirming the accuracy of the density calculations. This agreement supports the

validity of the force field, the application of periodic boundary conditions, and the model development for water-lean solvents.

Table 4. Density estimation in material studio's amorphous cell module.

Name of Solvent	Experimental Density (X_1) [47]	Simulation Density (X_2) Present Work	Std. Deviation
NMP	1.03	0.99	(-) 0.02
MEG	1.11	1.07	(-) 0.02
MDEA	1.10	1.05	(-) 0.025
MAE	0.940	0.945	(+) 0.0025
MeOH	0.80	0.79	(-) 0.005
Solvent System	Initial Density (X_1)	Final Density(X_2)	Std. Deviation
MDEA-MAE-EG	1.058	0.99	(-) 0.034
MDEA-EG	1.067	0.99	(-) 0.0385
MDEA-MAE-MeOH	1.002	0.90	(-) 0.051
MDEA-MeOH	1.007	0.89	(-) 0.0585
MDEA-MAE-NMP	1.044	0.92	(-) 0.062
MDEA-NMP	1.053	0.90	(-) 0.0765
MDEA-MAE	1.040	0.90	(-) 0.070

4. Result and Discussion

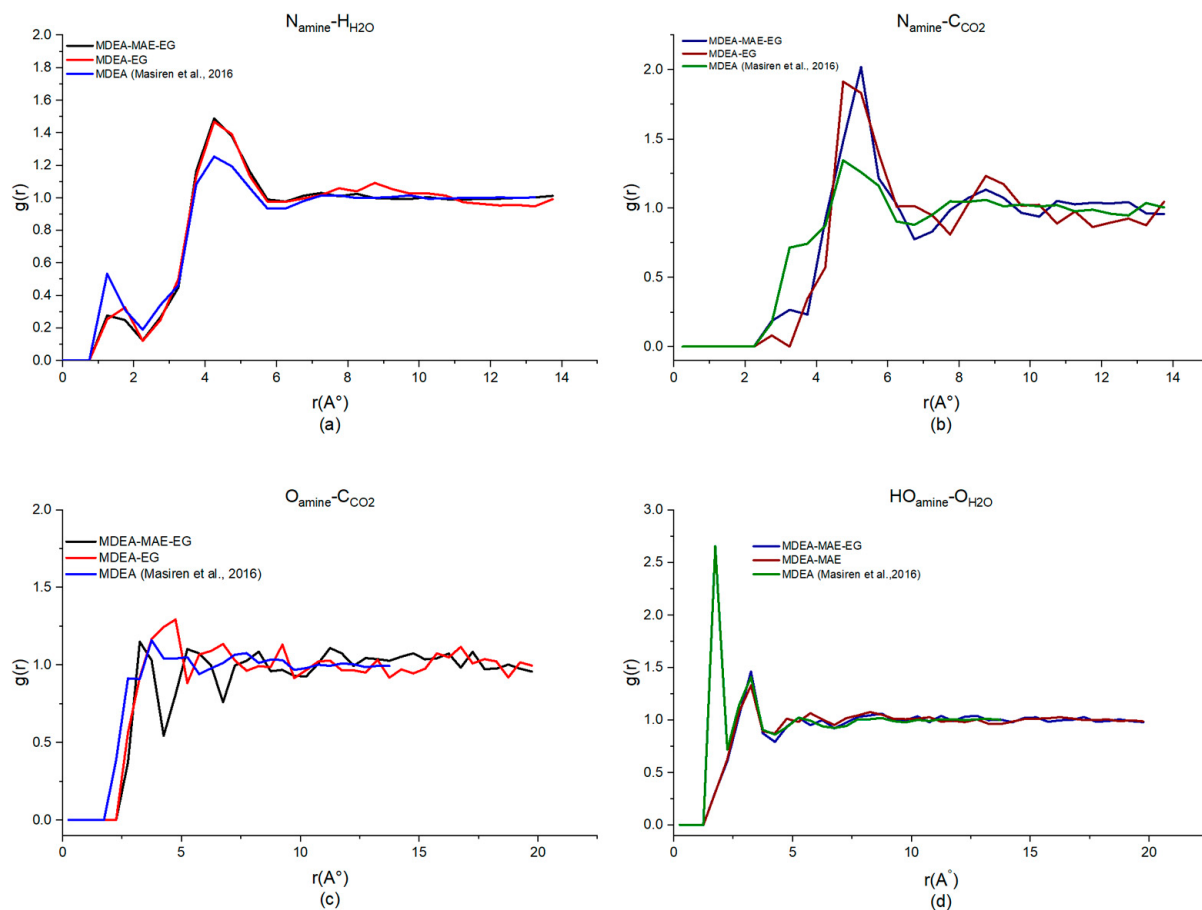
The RDF analysis for MDEA-NMP, MDEA-EG, MDEA-MeOH, and MDEA-MAE-NMP, MDEA-MAE-EG, and MDEA-MAE-MeOH has been conducted. Different blends of MDEA-MAE with co-solvents (Methanol, N-Methyl-2-pyrrolidone, and Monoethylene Glycol) reveal significant insights into their influence on amine-based solvent systems for CO_2 capture.

Table 5 shows the RDF results of various types of co-solvents with MDEA-MAE and the aqueous solvent of MDEA-MAE. The RDF (Radial Distribution Function) analysis findings for selected solvents in the study at 313 K provide insights into the interactions within MDEA-MAE and MDEA (N-methyldiethanolamine) systems with different solvents (MeOH, NMP, and EG) and varying water contents (30% and 50% H_2O). Figure 3 shows RDF findings in MDEA-MAE-EG and MDEA-EG and a comparison of MDEA-MAE-EG and MDEA-EG with pure MDEA. From Figure 3, it can be seen that $\text{N}_{\text{amine}}-\text{H}_{\text{H}_2\text{O}}$, $\text{N}_{\text{amine}}-\text{C}_{\text{CO}_2}$, and $\text{O}_{\text{amine}}-\text{C}_{\text{CO}_2}$ are higher in MDEA-EG compared to other systems. The other interaction, $\text{HO}_{\text{amine}}-\text{O}_{\text{H}_2\text{O}}$, is higher in aqueous MDEA. This can be due to the higher water concentration in MDEA, which indicates strong hydrogen bonding [49]. Similarly, Figure 4 shows the RDF findings of MDEA-MAE-MeOH and MDEA-MeOH. The interaction between $\text{N}_{\text{amine}}-\text{H}_{\text{H}_2\text{O}}$ and MDEA-MeOH is moderate, indicating good solvation. Overall, MDEA-MeOH shows moderate CO_2 capture and good solvation stability. Still, MDEA-MAE-MeOH shows stronger interaction with CO_2 with enhanced solvation and stability but a little weaker CO_2 solubility compared to MDEA-MeOH and aqueous MDEA (refer to Figure 4a-d). Therefore, we infer that MDEA-MAE-MeOH results are better than those of MDEA-MeOH and aqueous MDEA.

The other systems analyzed in the present work are MDEA-MAE-NMP and MDEA-NMP. Figure 5 shows the graphical representation of MDEA-MAE-NMP, MDEA-NMP, and aqueous MDEA. Compared to MDEA-MAE-NMP and MDEA-NMP, the MDEA-NMP system shows stronger interactions for all examined systems except $\text{HO}_{\text{amine}}-\text{O}_{\text{H}_2\text{O}}$. In fact, this interaction is highest in MDEA compared to all the solvent systems examined in the present work. Therefore, from the above discussion, we conclude that the MDEA-EG, MDEA-NMP, and MDEA-MAE-MeOH systems show prominent interaction intensity among all the observed systems.

Table 5. RDF analysis findings for selected solvents in the present study at 313 K.

System	Observed Interactions			
	N _{amine} -H _{H2O}	N _{amine} -C _{CO2}	O _{amine} -C _{CO2}	HO _{amine} -O _{H2O}
MDEA-NMP (40%H ₂ O)	4.75, 1.49	5.25, 1.90	5.25, 1.20	3.25, 1.37
MDEA-MAE-NMP (30%H ₂ O)	4.75, 1.31	5.25, 1.67	5.25, 1.21	3.25, 1.68
MDEA-EG (40%H ₂ O)	4.75, 1.47	4.75, 1.91	4.75, 1.29	3.25, 1.33
MDEA-MAE-EG (30%H ₂ O)	4.75, 1.22	5.25, 2.02	5.25, 1.10	3.25, 1.45
MDEA-MeOH (40%H ₂ O)	4.75, 1.44	5.25, 1.82	3.75, 1.43	3.25, 1.40
MDEA-MAE-MeOH (30%H ₂ O)	4.75, 1.53	5.25, 2.01	3.25, 0.92	3.25, 1.43
MDEA-MAE (50%H ₂ O)	4.75, 1.29	5.25, 1.67	5.25, 1.18	3.25, 1.35
MDEA [49,50]	4.25, 1.25	4.75, 1.34	3.75, 1.14	1.75, 2.65

**Figure 3.** Comparison of RDF Findings (a) N_{amine}-H_{H2O} (b) N_{amine}-C_{CO2} (c) O_{amine}-C_{CO2} (d) HO_{amine}-O_{H2O} in MDEA-MAE-EG and MDEA-EG with Aq. MDEA [50].

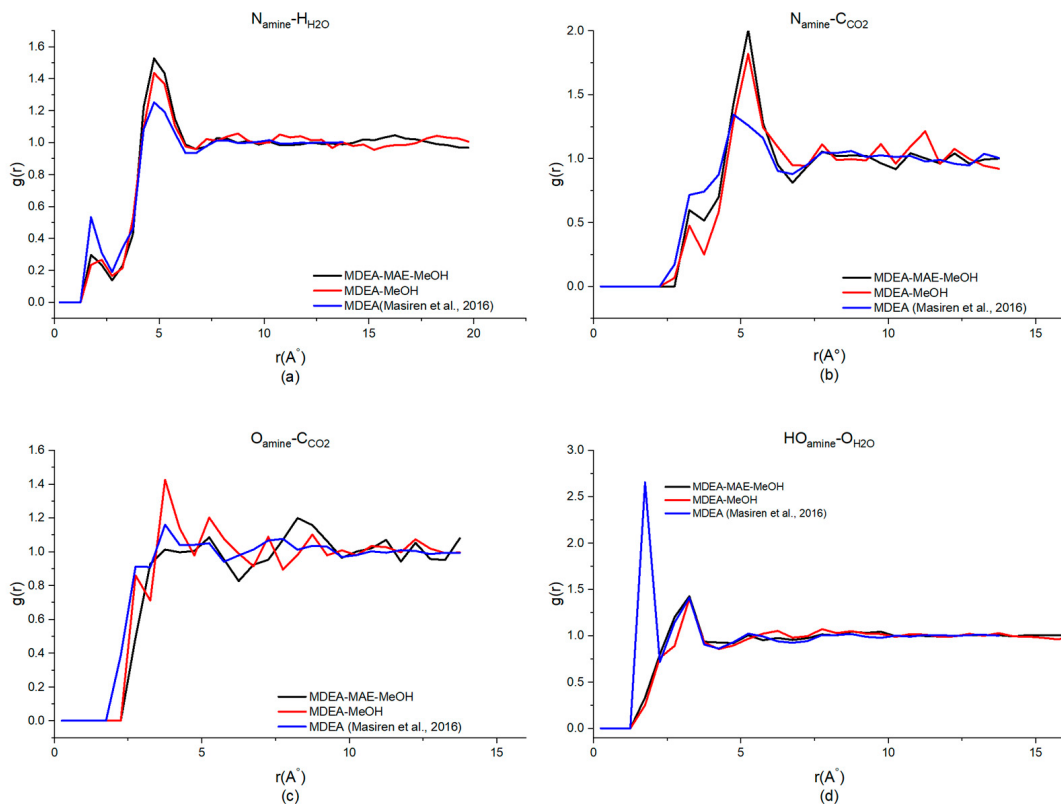


Figure 4. Comparison of RDF Findings (a) $\text{N}_{\text{amine}}-\text{H}_{\text{H}_2\text{O}}$ (b) $\text{N}_{\text{amine}}-\text{C}_{\text{CO}_2}$ (c) $\text{O}_{\text{amine}}-\text{C}_{\text{CO}_2}$ (d) $\text{HO}_{\text{amine}}-\text{O}_{\text{H}_2\text{O}}$ in MDEA-MAE-MeOH and MDEA-MeOH with Aq. MDEA [50].

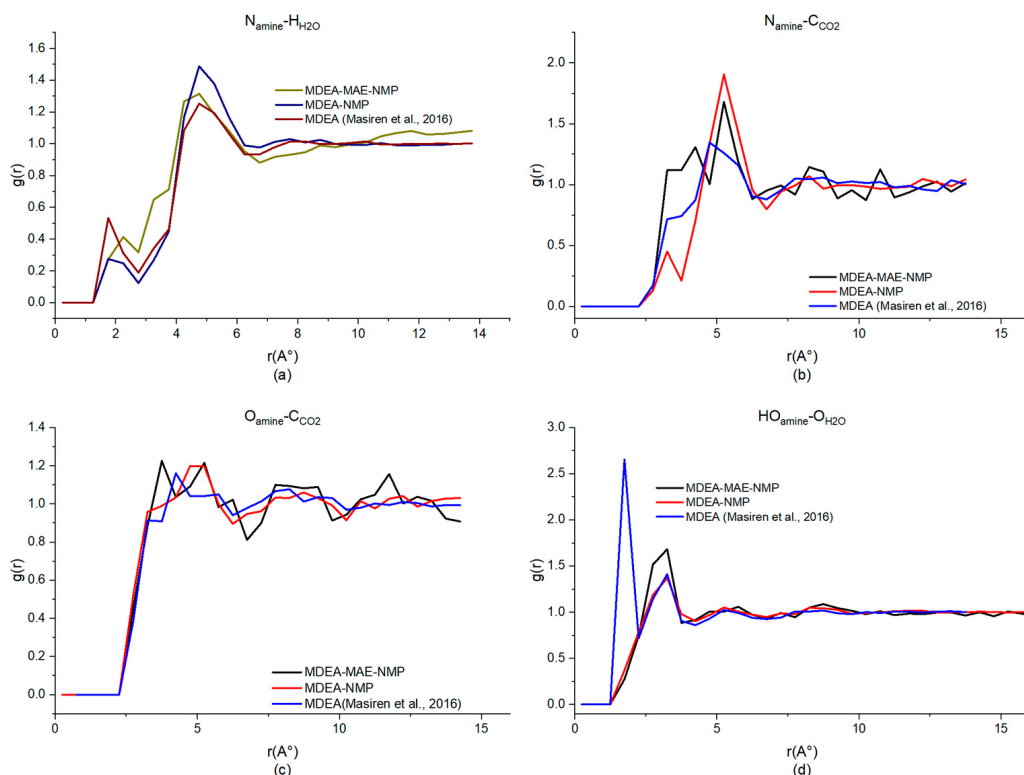


Figure 5. Comparison of RDF Findings (a) $\text{N}_{\text{amine}}-\text{H}_{\text{H}_2\text{O}}$ (b) $\text{N}_{\text{amine}}-\text{C}_{\text{CO}_2}$ (c) $\text{O}_{\text{amine}}-\text{C}_{\text{CO}_2}$ (d) $\text{HO}_{\text{amine}}-\text{O}_{\text{H}_2\text{O}}$ in MDEA-MAE-NMP and MDEA-NMP with Aq. MDEA [50].

A comparative analysis of the MDEA-MAE system with all three co-solvents will be conducted in the following discussion. Table 5 shows consistent distance $g(r)$ for RDF peak positions across different systems. However, the intensity of these peaks varies, indicating differences in interaction strengths. For example, in the $N_{\text{amine}}-\text{H}_2\text{O}$ (amine-water hydrogen bonding) interactions, the RDF peak position is consistently at 4.75 Å for all solvent systems, with variations in intensity: 1.53 Å for MeOH, 1.31 Å for NMP, and 1.22 Å for EG. This indicates a similar spatial arrangement but with varying interaction strengths, slightly stronger in MeOH. When the water content is increased to 50% (MDEA-MAE-50% H_2O without organic solvent), the RDF peak remains at 4.75 Å with an intensity of 1.29 Å, signifying a slight increase in hydrogen bonding interactions due to the higher water content. In the case of $N_{\text{amine}}-\text{CO}_2$ (amine-CO₂) interactions, all solvent systems show a consistent RDF peak at a distance (r) of 5.25 Å. The intensities, however, vary more significantly: 2.01 Å for MeOH, 1.67 Å for NMP, and 2.02 Å for EG. The interaction is strongest in the EG system, and the intensity decreases to 1.67 Å with 50% H_2O in the MDEA-MAE system. It indicates that the solvent system with EG (MDEA-MAE-EG) can enhance amine-CO₂ interactions.

For $O_{\text{amine}}-\text{CO}_2$ (oxygen in amine-CO₂) interactions, the RDF peaks were observed at 5.25 Å and 3.25 Å, with intensities showing notable differences: 3.25 Å, 0.92 Å for MeOH, 1.21 Å for NMP, and 1.10 Å for EG. The weakest interaction is observed in the MeOH system. With 50% H_2O , the intensity increases to 1.18 Å, highlighting the role of water in strengthening these interactions. Lastly, for $\text{HO}_{\text{amine}}-\text{OH}_2\text{O}$, the RDF peak is at 3.25 Å across all systems, with slight intensity variations: 1.43 Å for MeOH, 1.68 Å for NMP, and 1.45 Å for EG. The interaction strength decreases slightly in MeOH. With 50% H_2O , the intensity is 1.35 Å, indicating a moderate decrease in interaction strength with higher water content compared to MeOH and EG systems. Table 6 summarizes the co-solvent effect studied in the present work, and Table 7 shows the generalized findings of the study. The choice of water concentration and co-solvent significantly impacts the efficiency and stability of CO₂ capture systems. While lower water concentrations can enhance CO₂ interactions for some co-solvents, higher water concentrations generally provide more stable interactions. Optimizing these parameters is crucial for improving CO₂ capture performance. Moreover, the graphical representation of RDF is provided in the Supplementary Files.

Table 6. Summary of findings for various co-solvent effects and challenges.

Solvent System *	Interactions Results	Advantages	Challenges
Methanol	Strong CO ₂ interaction, slightly weaker solubility	Low molecular weight High solubility Effective interactions with amine and CO ₂ Enhances Hydrogen bonding	High Volatility Evaporation loss Handling issue [7,8]
N-Methyl-2-Pyrolidone	Improved stability and strong hydrogen bonds	High boiling point Strong solvation properties Improved stability for CO ₂ capture Higher interaction with CO ₂ Significantly enhances CO ₂ capture efficiency	Higher viscosity Affects flow properties Increased energy requirement for solvent circulation [48]
Ethylene Glycol	Strongest CO ₂ interaction, enhanced stability	Hygroscopic Nature Interaction shows High affinity for water Stable interactions Balances strong hydrogen bonding with effective CO ₂ capture	Higher molecular weight Potential viscosity issues [41]
MDEA-MAE-Aqueous Solvent	Moderate CO ₂ capture and stability	Increased hydrogen bonding with water Enhanced CO ₂ capture efficiency Stable interactions due to higher water content	Possible handling and processing challenges due to higher water content Higher energy requirement for solvent regeneration [49,51]

* Each solvent contains MDEA-MAE.

Table 7. General RDF findings with various co-solvents and water concentration at 313 K.

Co-Solvent	Water Concentration	Generalized Impact
NMP	30%H ₂ O and 40%H ₂ O	Exhibits stable CO ₂ interaction across different water concentrations, making it a versatile co-solvent.
EG	30%H ₂ O and 40%H ₂ O	Shows higher CO ₂ interaction at 40%H ₂ O, indicating better performance at higher water content but is temperature-sensitive.
MeOH	30%H ₂ O and 40%H ₂ O	Demonstrates higher CO ₂ interaction at 40%H ₂ O, but has handling challenges that must be managed.
MDEA-MAE (No Co-Solvent)	50%H ₂ O	Provides effective CO ₂ interactions with a good balance at 50%H ₂ O, but lower than with Co-solvent blends

5. Estimation of Diffusion Coefficient and Effect of Co-Solvent on CO₂ Diffusion in Various Aqueous and Water-Lean Solvent Systems

Table 8 presents the diffusivity estimation of CO₂ in different MDEA-MAE and MDEA-based solvent systems at three temperatures (313 K, 323 K, and 333 K). MSD analysis shows that diffusivity increases with an increase in temperature in the aqueous solvent MDEA-MAE (no organic co-solvents), i.e., 0.276×10^{-9} m²/s at 313 K, 0.477×10^{-9} m²/s at 323 K, and 0.660×10^{-9} m²/s at 333 K. It shows that diffusivity increases significantly with temperature, indicating that higher temperatures enhance the molecular motion and interaction between CO₂ and the solvent, thus improving CO₂ diffusion. A similar trend is observed in aqueous solvents in the literature as well as in our previous work [35,52,53]. This is because, at higher temperatures, the kinetic energy of the particle increases. As a result, the collision between particles increases, and we observe higher diffusivity. The other blend is MDEA-MAE with EG (30%H₂O) and MDEA-EG (40%H₂O). Unlike the other systems, this blend shows a decrease in diffusivity with an increase in temperature, as given in Figure 6c.

Table 8. Diffusivity estimation at various temperatures by MSD analysis.

Solvent System	CO ₂ Diffusivity (m ² .s ⁻¹)/Temperature		
	313 K	323 K	333 K
MDEA-NMP (40%H ₂ O)	2.51×10^{-9}	3.44×10^{-9}	4.47×10^{-9}
MDEA-MAE-NMP (30%H ₂ O)	0.210×10^{-9}	0.213×10^{-9}	0.202×10^{-9}
MDEA-MeOH (40%H ₂ O)	1.57×10^{-9}	2.47×10^{-9}	3.06×10^{-9}
MDEA-MAE-MeOH (30%H ₂ O)	0.308×10^{-9}	0.246×10^{-9}	0.413×10^{-9}
MDEA-EG (40%H ₂ O)	0.235×10^{-9}	0.350×10^{-9}	0.155×10^{-9}
MDEA-MAE-EG (30%H ₂ O)	0.284×10^{-9}	0.244×10^{-9}	0.1180×10^{-9}
MDEA-MAE (50%H ₂ O)	0.276×10^{-9}	0.477×10^{-9}	0.660×10^{-9}
50wt%MDEA	0.62×10^{-9} (298 K)	1.20×10^{-9} (313 K)	1.80×10^{-9} (323 K)
CO ₂ in pure H ₂ O	1.61×10^{-9} (298 K)	2.66×10^{-9} (313 K)	3.78×10^{-9} (323 K)

This could be due to the higher viscosity of EG [48]. MDEA-MAE-EG contains 30%H₂O, and we observe a decrease in diffusivity with an increase in temperature. Still, when the water concentration increased to 40% in MDEA-EG-40%H₂O, the diffusivity increased with an increase in temperature from 313 K to 323 K. This indicates that higher water concentrations reduce the viscosity of the solvent system, and we observe higher diffusivity. But 333 K again shows a decrease in diffusivity, which means the system's viscosity increases at higher temperatures. The effect can also be from the MDEA, because

a similar effect is observed in the case of pure MDEA. A study conducted by Al-Gawaas et al. (1989) shows that in the case of pure MDEA, viscosity decreases with an increase in temperature [54]. Molecular interactions also play a significant role. The presence of co-solvents like NMP, EG, and MeOH introduces additional hydrogen bonding, dipole-dipole interactions, and van der Waals forces. These interactions change non-linearly with temperature, leading to irregular diffusivity patterns [55]. This sensitivity can result in varying degrees of interaction strength at different temperatures, further complicating the diffusivity behavior. Viscosity changes with temperature also contribute to the irregular pattern. While temperature typically reduces viscosity, which should increase diffusivity, in co-solvent systems, the reduction in viscosity is not uniform across all components. This inconsistency leads to complex and non-linear changes in diffusivity. The other reason could be the presence of MAE. It can be seen from Table 8 that the presence of MAE reduces diffusivity compared to blends without MAE. This is because in MAE, due to relatively strong intermolecular forces, like hydrogen bonding, the molecules are organized and tightly packed, which increases the viscosity and surface tension and, as a result, decreases the diffusivity [46].

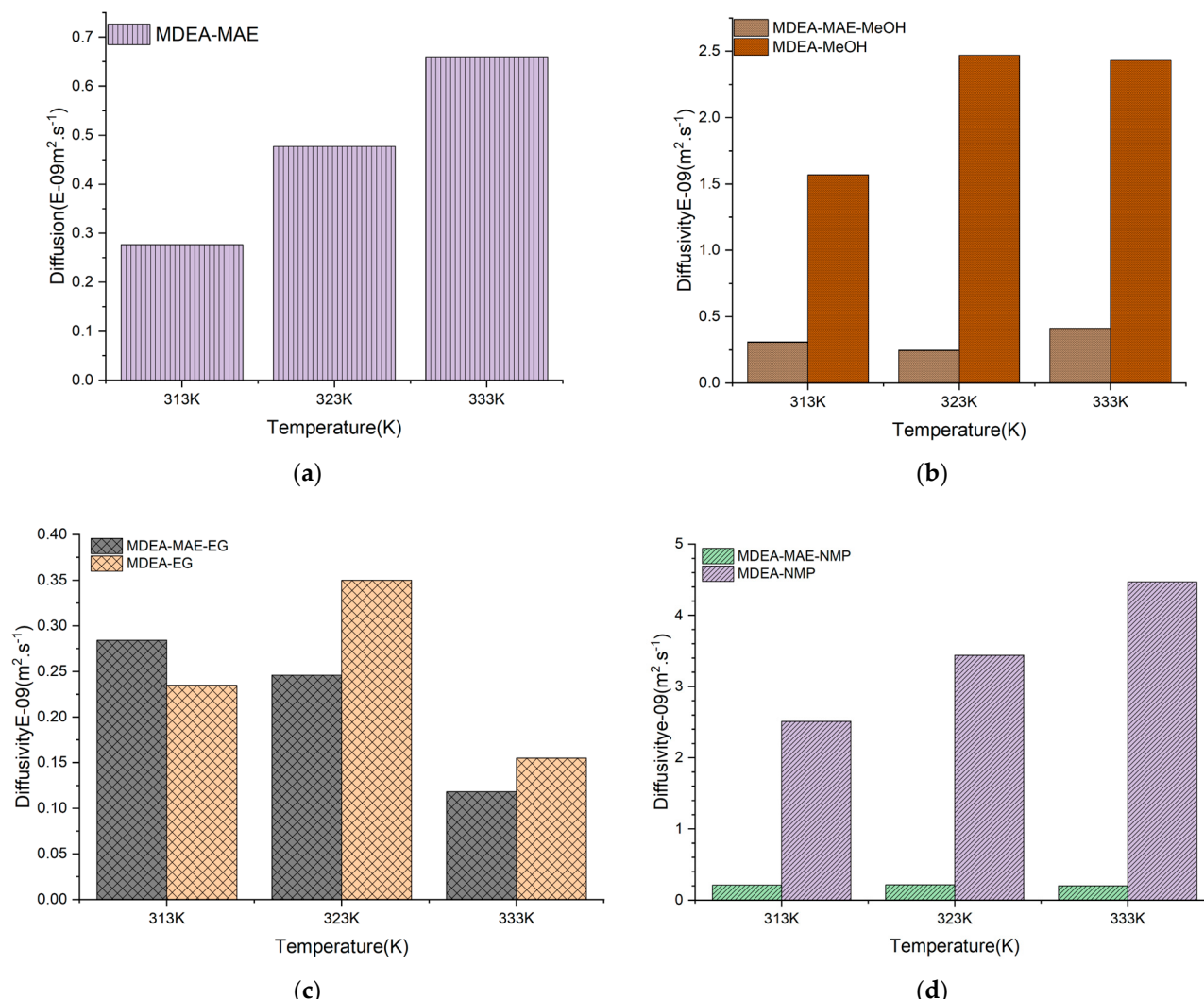


Figure 6. Comparison of CO₂ diffusivity ($\text{m}^2 \cdot \text{s}^{-1}$) estimation in (a) MDEA-MAE, (b) MDEA-MAE-MeOH, MDEA-MeOH, (c) MDEA-MAE-EG, MDEA-EG, (d) MDEA-MAE-NMP, and MDEA-NMP at three different temperatures.

The diffusivity trend in MDEA-MAE with NMP (30%H₂O) is 0.2108×10^{-9} m²/s at 313 K, 0.2139×10^{-9} m²/s at 323 K, and 0.2025×10^{-9} m²/s at 333 K (Figure 6d). The diffusivity values remain relatively constant across the temperature range, suggesting that NMP maintains a stable environment for CO₂ diffusion, potentially due to its high boiling point and consistent viscosity. On the other side, the blend without MAE (MDEA-NMP-40%H₂O) shows very high diffusivity compared to the MDEA-MAE-NMP-30%H₂O blend. This indicates that NMP shows different trends in both cases, each having a different water concentration. The literature can support these results. The studies show that NMP behaves differently with different water concentrations. For example, a study conducted by Xu et al. (2022) analyzed the diffusivity in MEA-NMP and DMPAD-NMP systems with varying water concentrations [56]. The results indicated that in the case of MEA-NMP, the diffusivity increases with an increase in temperature and water concentration, but in DMEDA-NMP and DMPDA-NMP systems, it shows an opposite trend (decreases with an increase in temperature and water concentration). Both of these blends containing NMP show different trends in diffusivity at three different temperatures.

The other systems analyzed in the present work are MDEA-MAE with MeOH (30%H₂O) and MDEA-MeOH (40%H₂O). The CO₂ diffusion coefficient in MDEA-MAE-MeOH is 0.308×10^{-9} m²/s at 313 K, 0.246×10^{-9} m²/s at 323 K, and 0.413×10^{-9} m²/s at 333 K, whereas it is 1.57×10^{-9} m²/s at 313 K, 2.47×10^{-9} m²/s at 323 K, and 3.06×10^{-9} m²/s at 333 K, as presented in Table 7 and Figure 6b. The results show variable trends, with a decrease at 323 K followed by a significant increase at 333 K in the MDEA-MAE-MeOH system.

The other systems analyzed in the present work are MDEA-MAE with MeOH (30%H₂O) and MDEA-MeOH (40%H₂O). The CO₂ diffusion coefficient in MDEA-MAE-MeOH is 0.308×10^{-9} m²/s at 313 K, 0.246×10^{-9} m²/s at 323 K, and 0.413×10^{-9} m²/s at 333 K, whereas it is 1.57×10^{-9} m²/s at 313 K, 2.47×10^{-9} m²/s at 323 K, and 3.06×10^{-9} m²/s at 333 K, as presented in Table 8 and Figure 6b. The results show variable trends, with a decrease at 323 K followed by a significant increase at 333 K in the MDEA-MAE-MeOH system. On the other side, the blend of MDEA-MeOH-40%H₂O shows an increase in diffusivity with an increase in temperature. The increase in diffusivity is due to the presence of MDEA, because studies show that MDEA has high diffusivity [54]. The initial decrease in MDEA-MAE-MeOH might be due to methanol's volatility and changes in solvent structure, but the sharp increase at higher temperatures suggests improved CO₂ diffusion, likely due to reduced solvent viscosity [41].

To check the validity of the simulation results, the CO₂ diffusivity in MDEA at 50 wt% and the CO₂ diffusivity in water were also examined. Table 9 compares the results of the present study with those of the literature. The graphical representation is provided in Figure 7. The detailed MSD analysis with adjusted R² values for all the solvent systems, including MDEA and H₂O at various temperatures, is given in the Supplementary Files. Table 9 represents the diffusivity estimation results as well as the density of the solvent system at various temperatures. It can be seen that the diffusivity of CO₂ in water is much higher than MDEA. The trend in diffusivity is the same in both MDEA and H₂O; it increases with an increase in temperature (Figure 7a,b). From the findings of the present work, there is a good agreement between the present study and the experimental studies in the literature, which can help validate the simulation results and research route adopted in the present study.

Selecting the appropriate co-solvent is crucial for optimizing the efficiency of amine-based CO₂ capture systems. Each co-solvent offers distinct advantages. The present research shows that methanol is suitable for applications requiring strong hydrogen bonding and effective CO₂ capture at lower temperatures, despite handling challenges. NMP shows consistent behavior at three different temperatures. Therefore, it is ideal for consistent performance across various temperatures with minimal evaporation losses [7,51]. EG Offers a balanced approach with strong hydrogen bonding and effective CO₂ capture, though its performance is temperature-sensitive. Generally, higher temperatures increase

diffusivity by enhancing molecular interactions and decreasing solvent viscosity, except for specific interactions observed in the EG system. Each co-solvent impacts the diffusivity differently, demonstrating the importance of selecting an appropriate co-solvent based on the desired temperature and diffusion characteristics [7,57]. EG shows unusual trends, potentially due to increased viscosity at higher temperatures and lower solubility [58]. NMP maintains stable diffusivity, making it a good candidate for systems requiring consistent performance across temperature variations. MeOH exhibits variability, indicating its performance is highly temperature-dependent [57]. The co-solvent and operating temperature choices profoundly affect CO₂ diffusivity in MDEA-MAE systems. Understanding these interactions helps in optimizing solvent formulations for efficient CO₂ capture. For stable and consistent diffusivity, NMP is favorable, whereas MEG and MeOH offer specific advantages at a particular temperature range.

Table 9. Comparison of CO₂ diffusivity ($\text{m}^2 \cdot \text{s}^{-1}$) with the literature at three different temperatures.

System	MDEA-50wt%			Reference
Temperature (K)	298	313	323	
CO ₂ Diffusivity in MDEA-50wt% ($\text{m}^2 \cdot \text{s}^{-1}$)	0.622×10^{-9} 0.624×10^{-9}	1.214×10^{-9} 1.204×10^{-9}	1.68×10^{-9} 1.70×10^{-9}	[54]
Density ($\text{g} \cdot \text{mL}^{-1}$) of MDEA mixture	1.0427 1.047	1.0331 1.047	1.0269 1.047	This work [54]
System		Pure H ₂ O		Reference
CO ₂ Diffusivity ($\text{m}^2 \cdot \text{s}^{-1}$) in H ₂ O	1.93×10^{-9} 1.61×10^{-9}	2.71×10^{-9} 2.66×10^{-9}	3.34×10^{-9} 3.78×10^{-9}	[54]
Density of mixture ($\text{g} \cdot \text{mL}^{-1}$)	0.9970 1.00	0.9922 1.00	0.9880 1.00	This work [54]
				This work

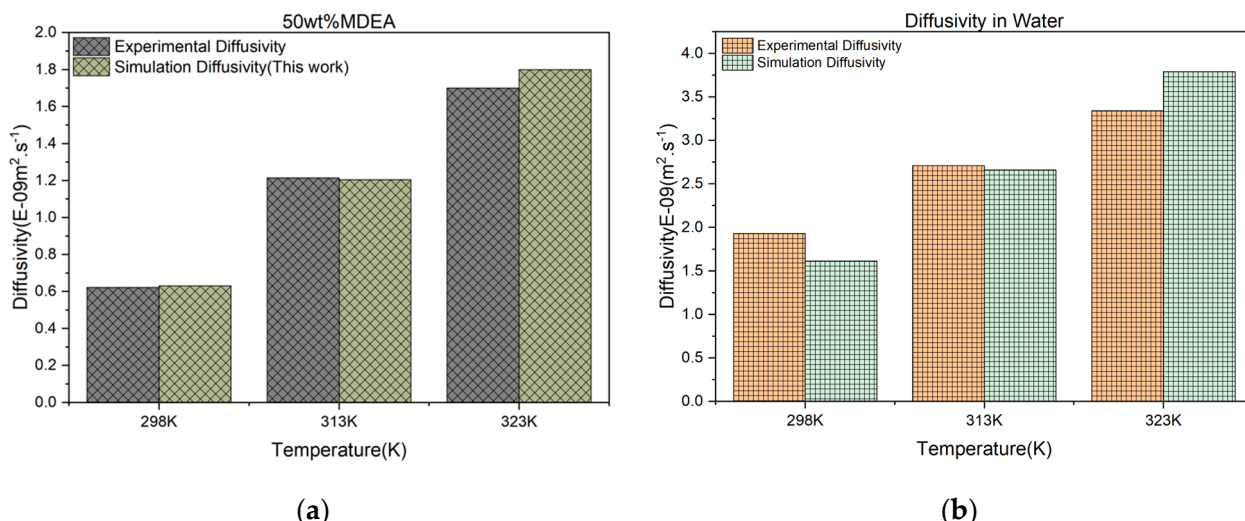


Figure 7. Comparison of (a) CO₂ diffusivity ($\text{m}^2 \cdot \text{s}^{-1}$) in MDEA and (b) in H₂O from the present work with the literature [54].

Our findings provide vital insights into the effect of various co-solvents on CO₂ capture efficiency, opening the path for developing more effective and sustainable CO₂ capture devices. Our findings demonstrate the potential of methanol, NMP, and EG as co-solvents, allowing for further steps such as solvent formulation optimization and laboratory-scale experiment design to test and develop these formulations. While keeping in mind the boundaries of the present work, the study's limitations include the fact that molecular dynamics simulations rely on force fields and approximations that may not fully capture

real-world complexities. In other words, the simulations were conducted only at specific temperatures, concentrations, and pressures, limiting extrapolation to other conditions.

6. Conclusions

The choice of co-solvent significantly impacts the performance of amine-based CO₂ capture systems. Understanding the specific interactions and properties of each co-solvent makes it possible to tailor the solvent system to meet the desired efficiency, stability, and cost-effectiveness, thereby optimizing the overall CO₂ capture process. The present study employed molecular dynamic simulation to assess the effect of co-solvent on CO₂ absorption and CO₂ diffusion in a water-lean MDEA-based solvent system using three types of organic solvents: NMP, MeOH, EG (MDEA-MAE-NMP, MDEA-MAE-MeOH, and MDEA-MAE-EG). MDEA-MAE (50%H₂O) without co-solvent is selected to check the effect of co-solvent. The effect of co-solvent was studied in two aspects: first, the effect on CO₂ absorption by RDF analysis, and second, the effect on CO₂ diffusion by MSD analysis.

The RDF analysis reveals that adding MAE does not raise the interaction intensity except in the MDEA-MAE-MeOH system. This system shows a slight rise in intensity compared to the MDEA-MeOH system. Specific interactions vary depending on the co-solvent used. Ethylene glycol (EG) and N-methyl-2-pyrollidone (NMP) show distinct behaviors in combination with MDEA and MAE. From all the observed systems, MDEA-EG (40%H₂O) and MDEA-NMP (40%H₂O) show higher intensity compared to other solvent systems examined in the present work, suggesting their potential as effective solvents for CO₂ capture. MDEA-MAE-50%H₂O (without co-solvent) shows lower interaction intensity compared to solvent systems with organic co-solvents. Similarly, the CO₂ diffusivity in this blend (MDEA-MAE-50%H₂O) is lower than in other water-lean solvents. However, it shows a regular trend in diffusivity with an increase in temperature.

The findings of CO₂ diffusivity estimation with different co-solvents combined with an MDEA-based system indicated that MDEA-NMP-40%H₂O and MDEA-EG-40%H₂O show the highest diffusivity in all the solvent systems examined in the present work. These systems exhibited higher CO₂ diffusivity across a range of temperatures (313 K, 323 K, and 333 K), indicating enhanced mobility and capture efficiency, particularly notable in MDEA-NMP (40%H₂O). In contrast, introducing MAE into these solvent blends generally weakened interaction intensities and CO₂ diffusivity, implying a less favorable impact on CO₂ capture efficiency than MDEA systems or those incorporating ethanol or ethylene glycol. This effect can be due to the stronger interactions in MAE because the organized and tightly packed molecules increase the viscosity and, as a result, decrease diffusivity. Furthermore, the temperature dependence of CO₂ diffusivity displayed complex behaviors in co-solvent systems compared to aqueous systems. The CO₂ diffusivity increases with the increase in temperature in the aqueous solvent MDEA-MAE, but the solvent system containing different co-solvents does not follow a regular pattern. This inconsistency leads to complex and non-linear changes in diffusivity in the presence of co-solvents. These results emphasize the effects of solvent composition on CO₂ capture efficiency under varying thermal conditions.

Future research can explore a wider range of co-solvents to optimize CO₂ capture efficiency and sustainability and address the potential for reductions in corrosion and degradation by adding co-solvents. Studies under varying temperature and pressure conditions will help identify optimal operational settings. Additionally, assessing the long-term stability of co-solvent-enhanced systems is crucial for understanding degradation mechanisms.

Supplementary Materials: The following supporting information can be downloaded at: <https://www.mdpi.com/article/10.3390/pr12081588/s1>, Figure S1: MSD analysis of MDEA-MAE based system with Various Co-solvents, Figure S2: Diffusivity ($m^2 \cdot s^{-1}$) Estimation in Various blends at three different Temperatures Figure S3: Diffusivity ($m^2 \cdot s^{-1}$) Estimation in Various blends at three different Temperatures, Figure S4: MSD analysis of CO₂ Diffusivity ($m^2 \cdot s^{-1}$) Estimation in H₂O, Figure S5: MSD Analysis of MDEA-NMP at three different Temperatures, Figure S6: MSD Analysis of MDEA-EG at three different Temperatures, Figure S7: MSD Analysis of 50wt%MDEA at three

different Temperatures, Figure S8: RDF study of MDEA-MAE (a) O_{amine}-C_{CO2} and (b) HO_{amine}-O_{H2O} with different Co-Solvents, Figure S9: RDF study of MDEA-MAE based System (a) N_{amine}-H_{H2O} and (b) N_{amine}-C_{CO2} with different Co-solvents, Figure S10: Diffusivity ($m^2 \cdot s^{-1}$) Estimation in Various blends at three different Temperatures.

Author Contributions: Conceptualization, M.S. and T.W.; Methodology and Software, M.S.; Formal analysis, C.G.; Investigation and data curation, W.Z.; Writing—original draft preparation, M.S.; Review and editing, M.F., T.W. and X.G.; Supervision, T.W.; Project Administration and funding acquisition, T.W. & M.F. All authors have read and agreed to the published version of the manuscript.

Funding: This study was supported by the National Key R&D Program of China (2022YFB4101700), the Pioneer R&D Program of Zhejiang Province (2023C03016), and the Zhejiang Provincial Natural Science Foundation of China (DT23E060002).

Data Availability Statement: Data is provided in the form of Tables and Figures in the Paper as well as in the Supplementary Files.

Conflicts of Interest: Authors Chunliang Ge and Wei Zhang were employed by the company Zhejiang Zheneng Technology & Environment Group Co., Ltd. The remaining authors declare that the research was conducted in the absence of any commercial or financial relationships that could be construed as a potential conflict of interest. The Zhejiang Zheneng Technology & Environment Group Co., Ltd. had no role in the design of the study; in the collection, analyses, or interpretation of data; in the writing of the manuscript, or in the decision to publish the results.

References

1. Liu, J.; Qian, J.; He, Y. Water-lean triethylenetetramine/N, N-diethylethanolamine/n-propanol biphasic solvents: Phase-separation performance and mechanism for CO₂ capture. *Sep. Purif. Technol.* **2022**, *289*, 120740. [[CrossRef](#)]
2. Tan, Y.; Nookuea, W.; Li, H.; Thorin, E.; Yan, J. Property impacts on Carbon Capture and Storage (CCS) processes: A review. *Energy Convers. Manag.* **2016**, *118*, 204–222. [[CrossRef](#)]
3. Feng, Y.; Chen, J.; Luo, J. Life cycle cost analysis of power generation from underground coal gasification with carbon capture and storage (CCS) to measure the economic feasibility. *Resour. Policy* **2024**, *92*, 104996. [[CrossRef](#)]
4. Desai, B.H. United Nations Environment Programme (UNEP). *Yearb. Int. Environ. Law* **2020**, *31*, 319–325. [[CrossRef](#)]
5. Fernández, J.; Sotenko, M.; Derevschikov, V.; Lysikov, A.; Rebrov, E.V. A radiofrequency heated reactor system for post-combustion carbon capture. *Chem. Eng. Process. Process Intensif.* **2016**, *108*, 17–26. [[CrossRef](#)]
6. Rubin, E.S.; Davison, J.E.; Herzog, H. The cost of CO₂ capture and storage. *Int. J. Greenh. Gas Control* **2015**, *40*, 378–400. [[CrossRef](#)]
7. Wanderley, R.R.; Pinto, D.D.; Knuutila, H.K. From hybrid solvents to water-lean solvents—A critical and historical review. *Sep. Purif. Technol.* **2021**, *260*, 118193. [[CrossRef](#)]
8. Heldebrant, D.J.; Koech, P.K.; Glezakou, V.-A.; Rousseau, R.; Malhotra, D.; Cantu, D.C. Water-lean solvents for post-combustion CO₂ capture: Fundamentals, uncertainties, opportunities, and outlook. *Chem. Rev.* **2017**, *117*, 9594–9624. [[CrossRef](#)]
9. Ping, T.; Dong, Y.; Shen, S. Energy-efficient CO₂ capture using nonaqueous absorbents of secondary alkanolamines with a 2-butoxyethanol cosolvent. *ACS Sustain. Chem. Eng.* **2020**, *8*, 18071–18082. [[CrossRef](#)]
10. Wanderley, R.R.; Pinto, D.D.; Knuutila, H.K. Investigating opportunities for water-lean solvents in CO₂ capture: VLE and heat of absorption in water-lean solvents containing MEA. *Sep. Purif. Technol.* **2020**, *231*, 115883. [[CrossRef](#)]
11. Wang, N.; Peng, Z.; Gao, H.; Sema, T.; Shi, J.; Liang, Z. New insight and evaluation of secondary Amine/N-butanol biphasic solutions for CO₂ Capture: Equilibrium Solubility, phase separation Behavior, absorption Rate, desorption Rate, energy consumption and ion species. *Chem. Eng. J.* **2022**, *431*, 133912. [[CrossRef](#)]
12. Shi, X.; Li, C.; Guo, H.; Shen, S. Density, viscosity, and excess properties of binary mixtures of 2-(methylamino) ethanol with 2-methoxyethanol, 2-ethoxyethanol, and 2-butoxyethanol from 293.15 to 353.15 K. *J. Chem. Eng. Data* **2019**, *64*, 3960–3970. [[CrossRef](#)]
13. Guo, H.; Li, C.; Shi, X.; Li, H.; Shen, S. Nonaqueous amine-based absorbents for energy efficient CO₂ capture. *Appl. Energy* **2019**, *239*, 725–734. [[CrossRef](#)]
14. Alkhatab, I.I.; Pereira, L.M.; AlHajaj, A.; Vega, L.F. Performance of non-aqueous amine hybrid solvents mixtures for CO₂ capture: A study using a molecular-based model. *J. CO₂ Util.* **2020**, *35*, 126–144. [[CrossRef](#)]
15. Wang, Z.; Yang, P.; He, X.; Yu, Q. Preparation of intercalated MXene by TPAOH and its adsorption characteristics towards U (VI). *J. Radioanal. Nucl. Chem.* **2024**, *333*, 1999–2014. [[CrossRef](#)]
16. Garcia, M.; Knuutila, H.K.; Aronu, U.E.; Gu, S. Influence of substitution of water by organic solvents in amine solutions on absorption of CO₂. *Int. J. Greenh. Gas Control* **2018**, *78*, 286–305. [[CrossRef](#)]
17. Li, Y.; Cheng, J.; Hu, L.; Liu, J.; Zhou, J.; Cen, K. Phase-changing solution PZ/DMF for efficient CO₂ capture and low corrosiveness to carbon steel. *Fuel* **2018**, *216*, 418–426. [[CrossRef](#)]
18. Ye, J.; Jiang, C.; Chen, H.; Shen, Y.; Zhang, S.; Wang, L.; Chen, J. Novel biphasic solvent with tunable phase separation for CO₂ capture: Role of water content in mechanism, kinetics, and energy penalty. *Environ. Sci. Technol.* **2019**, *53*, 4470–4479. [[CrossRef](#)]

19. Lin, Y.-J.; Pan, T.-H.; Wong, D.S.-H.; Jang, S.-S.; Chi, Y.-W.; Yeh, C.-H. Plantwide control of CO₂ capture by absorption and stripping using monoethanolamine solution. *Ind. Eng. Chem. Res.* **2011**, *50*, 1338–1345. [[CrossRef](#)]
20. Park, Y.; Lin, K.-Y.A.; Park, A.-H.A.; Petit, C. Recent advances in anhydrous solvents for CO₂ capture: Ionic liquids, switchable solvents, and nanoparticle organic hybrid materials. *Front. Energy Res.* **2015**, *3*, 42. [[CrossRef](#)]
21. Wang, R.; Liu, S.; Wang, L.; Li, Q.; Zhang, S.; Chen, B.; Jiang, L.; Zhang, Y. Superior energy-saving splitter in monoethanolamine-based biphasic solvents for CO₂ capture from coal-fired flue gas. *Appl. Energy* **2019**, *242*, 302–310. [[CrossRef](#)]
22. Li, Q.; Gao, G.; Wang, R.; Zhang, S.; An, S.; Wang, L. Role of 1-methylimidazole in regulating the CO₂ capture performance of triethylenetetramine-based biphasic solvents. *Int. J. Greenh. Gas Control* **2021**, *108*, 103330. [[CrossRef](#)]
23. Hu, H.; Fang, M.; Liu, F.; Wang, T.; Xia, Z.; Zhang, W.; Ge, C.; Yuan, J. Novel alkanolamine-based biphasic solvent for CO₂ capture with low energy consumption and phase change mechanism analysis. *Appl. Energy* **2022**, *324*, 119570. [[CrossRef](#)]
24. Chronopoulos, T.; Fernandez-Diez, Y.; Maroto-Valer, M.M.; Ocone, R.; Reay, D.A. CO₂ desorption via microwave heating for post-combustion carbon capture. *Microporous Mesoporous Mater.* **2014**, *197*, 288–290. [[CrossRef](#)]
25. Qian, J.; Sun, R.; Sun, S.; Gao, J. Computer-Free Group-Addition Method for p K a Prediction of 73 Amines for CO₂ Capture. *J. Chem. Eng. Data* **2017**, *62*, 111–122. [[CrossRef](#)]
26. El Hadri, N.; Quang, D.V.; Goetheer, E.L.; Zahra, M.R.A. Aqueous amine solution characterization for post-combustion CO₂ capture process. *Appl. Energy* **2017**, *185*, 1433–1449. [[CrossRef](#)]
27. Barzaghi, F.; Mani, F.; Peruzzini, M. A comparative study of the CO₂ absorption in some solvent-free alkanolamines and in aqueous monoethanolamine (MEA). *Environ. Sci. Technol.* **2016**, *50*, 7239–7246. [[CrossRef](#)]
28. Liu, B.; Luo, X.; Gao, H.; Idem, R.; Tontiwachwuthikul, P.; Olson, W.; Liang, Z. Reaction kinetics of the absorption of carbon dioxide (CO₂) in aqueous solutions of sterically hindered secondary alkanolamines using the stopped-flow technique. *Chem. Eng. Sci.* **2017**, *170*, 16–25. [[CrossRef](#)]
29. Bihong, L.; Kexuan, Y.; Xiaobin, Z.; Zuoming, Z.; Guohua, J. 2-Amino-2-methyl-1-propanol based non-aqueous absorbent for energy-efficient and non-corrosive carbon dioxide capture. *Appl. Energy* **2020**, *264*, 114703. [[CrossRef](#)]
30. Tan, L.; Shariff, A.; Lau, K.; Bustam, M. Impact of high pressure on high concentration carbon dioxide capture from natural gas by monoethanolamine/N-methyl-2-pyrrolidone solvent in absorption packed column. *Int. J. Greenh. Gas Control* **2015**, *34*, 25–30. [[CrossRef](#)]
31. Henni, A.; Mather, A.E. Solubility of carbon dioxide in methyldiethanolamine+ methanol+ water. *J. Chem. Eng. Data* **1995**, *40*, 493–495. [[CrossRef](#)]
32. Wanderley, R.R.; Evjen, S.; Pinto, D.D.D.; Knuutila, H.K. The salting-out effect in some physical absorbents for CO₂ capture. *Chem. Eng. Trans.* **2018**, *69*, 97–102.
33. Schlecht, M.F. *Molecular Modeling on the PC*; Wiley-VCH: New York, NY, USA, 1998.
34. Li, Z.; Gan, B.; Li, Z.; Zhang, H.; Wang, D.; Zhang, Y.; Wang, Y. Kinetic mechanisms of methane hydrate replacement and carbon dioxide hydrate reorganization. *Chem. Eng. J.* **2023**, *477*, 146973. [[CrossRef](#)]
35. Narimani, M.; Amjad-Iranagh, S.; Modarress, H. Performance of tertiary amines as the absorbents for CO₂ capture: Quantum mechanics and molecular dynamics studies. *J. Nat. Gas Sci. Eng.* **2017**, *47*, 154–166. [[CrossRef](#)]
36. Song, Z.; Han, D.; Yang, M.; Huang, J.; Shao, X.; Li, H. Formic acid formation via direct hydration reaction (CO+ H₂O→ HCOOH) on magnesia-silver composite. *Appl. Surf. Sci.* **2023**, *607*, 155067. [[CrossRef](#)]
37. Sharif, M.; Fan, H.; Sultan, S.; Yu, Y.; Zhang, T.; Wu, X.; Zhang, Z. Evaluation of CO₂ absorption and stripping process for primary and secondary amines. *Mol. Simul.* **2023**, *49*, 565–575. [[CrossRef](#)]
38. Biovia. *Material Studio*, Biovia: 2019 Version; Available online: <https://www.3ds.com/products/biovia/materials-studio> (accessed on 24 July 2024).
39. Meunier, M. Diffusion coefficients of small gas molecules in amorphous cis-1, 4-polybutadiene estimated by molecular dynamics simulations. *J. Chem. Phys.* **2005**, *123*, 134906. [[CrossRef](#)]
40. Allen, M.P.; Tildesley, D.J. *Computer Simulation of Liquids*; Oxford University Press: Oxford, UK, 2017.
41. Zhang, G.; Liu, J.; Qian, J.; Zhang, X.; Liu, Z. Review of Research Progress and Stability Studies of Amine-based Biphasic Absorbents for CO₂ Capture. *J. Ind. Eng. Chem.* **2024**, *134*, 28–50. [[CrossRef](#)]
42. Shamiri, A.; Shafeeyan, M.; Tee, H.; Leo, C.; Aroua, M.; Aghamohammadi, N. Absorption of CO₂ into aqueous mixtures of glycerol and monoethanolamine. *J. Nat. Gas Sci. Eng.* **2016**, *35*, 605–613. [[CrossRef](#)]
43. Olyaei, E.; Hafizi, A.; Rahimpour, M. Low energy phase change CO₂ absorption using water-lean mixtures of glycine amino acid: Effect of co-solvent. *J. Mol. Liq.* **2021**, *336*, 116286. [[CrossRef](#)]
44. Versteeg, G.; van Swaaij, W.P.M. On the kinetics between CO₂ and alkanolamines both in aqueous and non-aqueous solutions—II. Tertiary amines. *Chem. Eng. Sci.* **1988**, *43*, 587–591. [[CrossRef](#)]
45. Laddha, S.; Danckwerts, P. Reaction of CO₂ with ethanolamines: Kinetics from gas-absorption. *Chem. Eng. Sci.* **1981**, *36*, 479–482. [[CrossRef](#)]
46. Matsubara, H.; Pichierri, F.; Kurihara, K. Mechanism of diffusion slowdown in confined liquids. *Phys. Rev. Lett.* **2012**, *109*, 197801. [[CrossRef](#)]
47. ChemsSpider. Royal Society of Chemistry Database. 2020. Available online: <https://www.chemspider.com/> (accessed on 24 July 2024).
48. Yaws, C.L. *Yaws' Thermophysical Properties of Chemicals and Hydrocarbons*; Knovel: New York, NY, USA, 2009.

49. Harun, N.; Masiren, E. Molecular dynamic simulation of amine-CO₂ absorption process. *Indian J. Sci. Technol.* **2017**, *10*. [CrossRef]
50. Masiren, E.; Harun, N.; Ibrahim, W.; Adam, F. Intermolecular Interaction of Monoethanolamine, Diethanolamine, Methyl diethanolamine, 2-Amino-2-methyl-1-propanol and Piperazine Amines in Absorption Process to Capture CO₂ using Molecular Dynamic Simulation Approach. Universiti Malasiya Pahang. *The National Conference for Postgraduate Research*. 2016. Available online: <http://umpir.ump.edu.my/id/eprint/15835/1/P053%20pg385-397.pdf> (accessed on 24 July 2024).
51. Yuan, Y.; Rochelle, G.T. CO₂ absorption rate in semi-aqueous monoethanolamine. *Chem. Eng. Sci.* **2018**, *182*, 56–66. [CrossRef]
52. Sharif, M.; Han, T.; Wang, T.; Shi, X.; Fang, M.; Shuming, D.; Meng, R.; Gao, X. Investigation of Rational Design of Amine Solvents for CO₂ Capture: A Computational Approach. *Chem. Eng. Res. Des.* **2024**, *204*, 524–535. [CrossRef]
53. Sharif, M.; Wang, T.; Xu, Y.; Fang, M.; Wu, H.; Gao, X. Evaluating solvent efficiency for carbon capture: Comparative analysis of temperature, concentration and diffusivity effects. *Geoenergy Sci. Eng.* **2024**, *237*, 212833. [CrossRef]
54. Al-Ghawas, H.A.; Hagewiesche, D.P.; Ruiz-Ibanez, G.; Sandall, O.C. Physicochemical properties important for carbon dioxide absorption in aqueous methyldiethanolamine. *J. Chem. Eng. Data* **1989**, *34*, 385–391. [CrossRef]
55. Varady, M.J.; Knox, C.K.; Cabalo, J.B.; Bringuer, S.A.; Pearl, T.P.; Lambeth, R.H.; Mantooth, B.A. Molecular dynamics study of competing hydrogen bonding interactions in multicomponent diffusion in polyurethanes. *Polymer* **2018**, *140*, 140–149. [CrossRef]
56. Xu, Y.; Yang, Q.; Puxty, G.; Yu, H.; Conway, W.; Fang, M.; Wang, T.; Mulder, R.J. Diffusivity in Novel Diamine-Based Water-Lean Absorbent Systems for CO₂ Capture Applications. *Ind. Eng. Chem. Res.* **2022**, *61*, 12493–12503. [CrossRef]
57. Park, S.-W.; Lee, J.-W.; Choi, B.-S.; Lee, J.-W. Absorption of carbon dioxide into non-aqueous solutions of N-methyldiethanolamine. *Korean J. Chem. Eng.* **2006**, *23*, 806–811. [CrossRef]
58. Xu, H.-J.; Zhang, C.-F.; Zheng, Z.-S. Solubility of hydrogen sulfide and carbon dioxide in a solution of methyldiethanolamine mixed with ethylene glycol. *Ind. Eng. Chem. Res.* **2002**, *41*, 6175–6180. [CrossRef]

Disclaimer/Publisher's Note: The statements, opinions and data contained in all publications are solely those of the individual author(s) and contributor(s) and not of MDPI and/or the editor(s). MDPI and/or the editor(s) disclaim responsibility for any injury to people or property resulting from any ideas, methods, instructions or products referred to in the content.